Eur. Phys. J. B **31**, 457–461 (2003)
DOI: 10.1140/epjb/e2003-00055-1

THE EUROPEAN PHYSICAL JOURNAL B

Macroscopic oscillations between two weakly coupled Bose-Einstein condensates

A. Smerzi[1,2,a], A. Trombettoni[1,2], T. Lopez-Arias[3], C. Fort[1,3], P. Maddaloni[1,3], F. Minardi[1,3], and M. Inguscio[1,3]

[1] Istituto Nazionale di Fisica della Materia, Italy
[2] International School for Advanced Studies (SISSA), via Beirut 2/4, 34014 Trieste, Italy
[3] European Laboratory for Non-Linear Spectroscopy (LENS), Largo E. Fermi 2, 50125 Firenze, Italy

Received 2 May 2002 / Received in final form 19 November 2002
Published online 6 March 2003 –

Abstract. We demonstrate, both from a theoretical and an experimental point of view, the possibility of realizing a weak coupling between two Bose-Einstein condensates trapped in different Zeeman states. The weak coupling drives macroscopic quantum oscillations between the condensate populations and the observed current-phase dynamics is described by generalized Josephson equations. In order to highlight the superfluid nature of the oscillations, we investigate the response of a ^{87}Rb non-condensate (thermal) gas in the same conditions, showing that the thermal oscillations damp more quickly than those of the condensate.

PACS. 03.75.Fi Phase coherent atomic ensembles; quantum condensation phenomena – 05.30.Jp Boson systems

The Josephson effect

The manifestation of phase coherence on macroscopic scales is among the most spectacular phenomena occurring in superfluids and superconductors [1]. According to quantum mechanics, only the relative phase between two of such quantum systems is observable, while the phase of a single one is not. If a *weak link* is created between two quantum fluids, as a small perturbation on the uncoupled systems, a particle current driven by the relative phase oscillates through the junction, providing a non-destructive test of phase coherence. This is at the heart of the Josephson effect (JE), predicted in the sixties [2], and verified experimentally with superconductors [3], superfluid helium [4,5] and arrays of BECs [6,7].

From the historical point of view, the first weak link achieved was a tunneling barrier between two superconducting systems. Soon after, it was realized that tunneling was just one way among others to create a weak link, and "contact junctions" (with the two superconducting systems sharing a small area) were implemented [3]. In neutral superfluids, the search for the JE has been problematic due to the difficulty of creating weak links. Evidences for Josephson oscillations across a micropore connecting two ^{3}He-B baths were reported by Avenel and Varoquaux [4] and their first direct observation has been recently reported by Davis, Packard and collaborators [5]. The weak link was provided by the spatial overlap of the two superfluid wavefunction tails inside the micropore. For BECs, multiple connected weak links have been realized with optical lattices: by using two counterpropagating lasers, a periodic potential acts on the atomic gas and a chain of weakly coupled BECs (*i.e.* an array of Josephson junctions) is created. Each junction is given by the condensates in neighbouring minima of the lattice potential, the weak link between them being provided by the energy barrier which is proportional to the laser power. Coherence between atomic waves tunneling from an array of weakly coupled BECs located at different heights in the earth's gravitational field, has been shown by Anderson and Kasevich [6]; a direct observation of the Josephson current in the array is reported in [7].

Up to date, the direct observation of a Josephson current between only *two* BECs has been more elusive. A possible way to create a junction is to divide an harmonic magnetic trap in two halves using a laser "chisel", creating an effective double well. However, the experimental difficulties associated with the stability and the spatial dimensions of the laser beam make this task difficult [8]. A further possibility is to consider two different internal hyperfine states: in this case the Josephson atomic current is between different spin states. It is rather common, in the literature, to refer to the latter case as the "internal" JE. In the "internal" JE the states which are weakly coupled differ by some intrinsic (spin) quantum number, and they are not necessarily separated spatially (as in the double well). An example of internal JE is the longitudinal

[a] e-mail: smerzi@sissa.it

magnetic resonance in superfluid $^3\mathrm{He}-\mathrm{A}$ [9]; in this case the relevant degree of freedom is the hyperfine (nuclear spin) index of a Cooper pair [10].

Josephson vs. Rabi

The crucial step to observe the Josephson effect is to create a weak link between two condensates. The JE is a non-destructive manifestation of phase coherence in a (macroscopic) quantum fluid. The idea is to couple the two fluids, and then inquire about their (if any) relative phase, without (and this is the crux) perturbing the bulk properties of the two systems. Of course, this implies that the energy scale of the coupling probe must be small as compared with the chemical potential of both fluids. The Rabi effect (RE), on the other hand, regards the manifestation of coherence between internal states in the single atom dynamics. In this respect the RE is a manifestation of quantum effects on a microscopic (atomic) scale. These quantum effects can be easily washed out by the incoherent collisions and other dephasing mechanisms in a gas of interacting atoms. Quite the contrary, the collective coherence of a condensate is expected to be naturally robust for the same reason, *i.e.* because of the interatomic interaction. As it is well known, the superfluid nature of the condensate can be related with the low energy excitation spectrum of the system, which is linear instead of quadratic, see for instance [1].

In this paper we suggest a scheme to create a weak link between two condensates trapped in different hyperfine levels and we report on its experimental realization. The weak link is provided by a strongly detuned radio-frequency (rf) field which couples the two spin states.

The experiment

A dilute gas of ^{87}Rb atoms is trapped and cooled below the critical temperature for Bose-Einstein condensation [11], $T_c \simeq 150$ nK, with a combination of laser and evaporative cooling. The atoms are confined by dc magnetic fields generated by a set of four coils, arranged so as to create an axially symmetric harmonic potential [12]. A single condensate in the Zeeman state $|F=2, m_F=2\rangle \equiv |2\rangle$ is created first. Subsequently, we apply a first strong (and very short) rf field to create a second condensate in the Zeeman state $|F=2, m_F=1\rangle \equiv |1\rangle$ (there is a small transfer of population into the other three accessible Zeeman levels that can be neglected in the dynamics of the system). The two equally populated condensates are fully overlapped in space. This gives our initial ($t=0$) configuration. Having different magnetic momenta, the atoms of the two species feel different trapping potentials $V_2 = \frac{1}{2}m\omega^2\{x^2 + l^2(y^2+z^2)\} + mgz$ and $V_1 = \frac{1}{4}m\omega^2\{x^2 + l^2(y^2+z^2)\} + mgz$ (with $\omega = 2\pi \times 12.6$ Hz, $l = 10.37$ the ratio between the axial and radial trap frequency, m the atomic mass and g the gravity acceleration constant). Therefore, they begin to separate from each other, each one following its own potential. In Figure 1 we report these potentials along the z-direction, in which the motion of the condensates effectively occurs: the centers of the two potentials are separated by approximately 15 μm (which is a large amount respect to the width of the condensates, 4.3 μm). In ≈ 500 μs the two condensates would get completely separated, but in the typical time scale of our experiment (≈ 100 μs), they are still almost completely overlapped and the motion of $|1\rangle$ is basically ballistic: in the typical time scale of the experiment $|1\rangle$ moves apart along the vertical z-axis at most by 0.02 μm. The two condensates then remain essentially overlapped and with no change in shape.

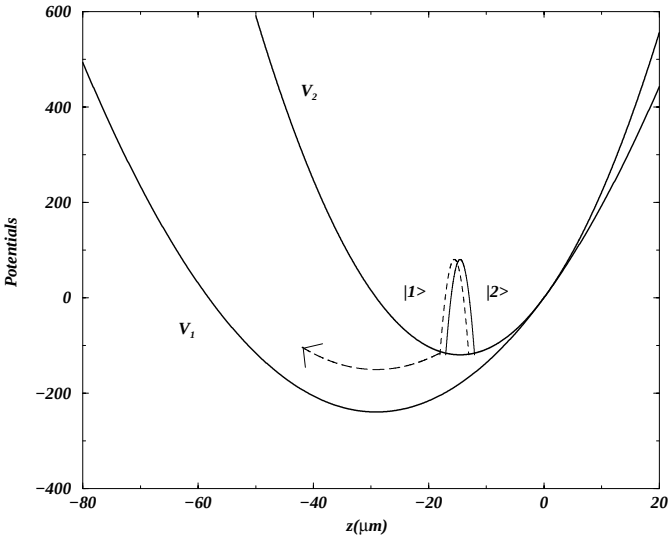

Fig. 1. Potentials (in unity of $\hbar\omega l$) felt by the two condensates along the z-axis, in which the motion effectively occurs. Initially the two condensates are completely overlapped (in the figure, the density profiles are slightly shifted and magnified for graphical clarity). The complete oscillations of the condensate $|1\rangle$ around its center have a period of order 10 ms: in the typical time scale of the experiment (≈ 100 μs), $|1\rangle$ moves at most of 0.02 μm and the two condensates remain essentially overlapped.

While the condensate $|1\rangle$ begins to move, in order to create the weak link between the two Zeeman states we turn on an external rf field $\hbar\Omega_R \mathrm{e}^{\mathrm{i}\omega_{rf}t}$ with detuning $\delta = \omega_{rf} - \omega_0$ ($\omega_0 \approx 2\pi \cdot 2$ MHz is the energy shift between the two Zeeman states in the minimum of the magnetic trap). The order parameters $\psi_j(\boldsymbol{r}, t)$ for the condensate j ($j = 1, 2$) obey, in the rotating wave approximation, a set of two-coupled Gross-Pitaevskii equations [13,14]:

$$\mathrm{i}\hbar \begin{pmatrix} \dot{\psi}_2 \\ \dot{\psi}_1 \end{pmatrix} = \begin{pmatrix} \hat{H}_2 - \hbar\delta/2 & \hbar\Omega_R/2 \\ \hbar\Omega_R/2 & \hat{H}_1 + \hbar\delta/2 \end{pmatrix} \begin{pmatrix} \psi_2 \\ \psi_1 \end{pmatrix} \qquad (1)$$

where $H_i = -\frac{\hbar^2}{2m}\nabla^2 + V_i + H_i^{MF}$. The mean-field interaction for each component is described by $H_i^{MF} = g_{ii}|\psi_i|^2 + g_{ij}|\psi_j|^2$ and it is characterized by $g_{ij} = 4\pi\hbar^2 a_{ij}/m$, which depends on the scattering length a_{ij} of the collision (there are three different values: a_{11}, a_{22}, a_{12}). The scattering

lengths are almost degenerate and the effective mean-field contribution to the chemical potential difference between the two condensates is of the order of 50 Hz.

The weak link

In [13] it has been suggested that a weak link can be created with $\delta = 0$ and Ω_R smaller than the shift between the trap energy levels (for typical values, it has to be $\Omega_R \sim 2\pi \times 10$ Hz). In this regime, the frequency of the oscillations is modified by the nonlinearity of GPE. However, the attempts to create such weak links are heavily obstructed because, for technical reasons, with such a small value of Ω_R the ratio signal/noise is too small to allow observing the Josephson oscillations. With a Rabi frequency $\Omega_R \gtrsim 0.5$ kHz, the mean-field contribution is negligible in the coupled dynamics.

Here we choose an alternative way to create the weak link: the detuning δ of the coupling external rf field is taken to be $\gg \Omega_R$. This is crucial in the present experiment: expanding the wave functions in the parameter $\Omega_R/2\delta$, the standard first order perturbation theory [15] correctly applies when this parameter is $\ll 1$. The GPE (1) can be written in the form $\mathrm{i}\hbar \begin{pmatrix} \dot{\psi}_2 \\ \dot{\psi}_1 \end{pmatrix} = (\hat{H}_0 + \hat{W}) \begin{pmatrix} \psi_2 \\ \psi_1 \end{pmatrix}$ where $\hat{H}_0 = \begin{pmatrix} \hat{H}_2 & 0 \\ 0 & \hat{H}_1 \end{pmatrix}$ and $\hat{W} = \frac{\hbar\delta}{2} \begin{pmatrix} -1 & \Omega_R/\delta \\ \Omega_R/\delta & 1 \end{pmatrix}$. If we neglect the mean-field term in the dynamics, as previously discussed, the Hamiltonians of the uncoupled systems (*i.e.* without the external e.m. field) are $\hat{H}_2 = -\frac{\hbar^2}{2m}\nabla^2 + V_2$ and $\hat{H}_1 = -\frac{\hbar^2}{2m}\nabla^2 + V_1$. A basis for $\hat{H}_0$ is given by $\left\{ \begin{pmatrix} \psi_{2n} \\ 0 \end{pmatrix}, \begin{pmatrix} 0 \\ \psi_{1m} \end{pmatrix} \right\}$ with $\hat{H}_2\psi_{2n} = E_{2n}\psi_{2n}$ and $\hat{H}_1\psi_{1m} = E_{1m}\psi_{1m}$. Applying the standard first order perturbation theory, we see that the correction to, for instance, the wavefunctions $\begin{pmatrix} \psi_{2n} \\ 0 \end{pmatrix}$ is given by

$$\begin{pmatrix} 0 \\ \sum_m \frac{\Omega_R \int \mathrm{d}\boldsymbol{r}\psi_{2m}\psi_{1n}}{2(E_{2m}-E_{1n}+\delta)}\psi_{2m} \end{pmatrix}$$

from which we can see the standard first order perturbation theory correctly applies when $\Omega_R/2\delta \ll 1$: in this condition, the external rf field is a weak link. We use in the experiment $\Omega_R = 2\pi \times 13$ kHz and $\delta = 2\pi \times 80$ kHz.

We notice that the dynamical regimes of weakly linked superfluids are often classified in the literature as [10]: 1) "Rabi" (for $K/E_J \ll N^{-2}$), 2) "Josephson" (for $N^{-2} \ll K/E_J \ll 1$), 3) "Fock" (for $K/E_J \gg 1$). N is the number of particles, $E_J = N\hbar\Omega_R$ is the Josephson energy of the junction and $K = \frac{4\pi\hbar^2}{m}(g_{11} + g_{22} - 2g_{12})\chi$, where $\chi = \int \mathrm{d}\boldsymbol{r}\Phi(\boldsymbol{r})^4$ and $\Phi(\boldsymbol{r})$ is the equilibrium condensate wavefunction. According to this classification we are in the "Rabi" case.

The Josephson equations

Since in the far-detuned regime the external field is a weak link, the condensates dynamics can be described in the two-mode approximation and the two wavefunctions can be parameterized (in the center of mass frame) as $\psi_j(\boldsymbol{r};t) = \sqrt{N_j(t)}\mathrm{e}^{\mathrm{i}\phi_j(t)}\ \Phi(\boldsymbol{r})\mathrm{e}^{\frac{\mathrm{i}}{\hbar}p_j(t)\cdot z}$: $\int \mathrm{d}\boldsymbol{r}|\psi_j|^2 = N_j$ is the number of particle of the condensate j, p_j is the condensate momentum and $\Phi(\boldsymbol{r})$ the $|2,2\rangle$ wavefunction at $t = 0$, (the condensed $|2\rangle$ is in equilibrium wavefunction before the application of the rf fields). The temporal evolution of $\Phi(\boldsymbol{r})$ can be neglected for the reason before discussed. Substituting in the equations (1), the equations of motion for the particle number N_j and its conjugate momentum ϕ_j, are

$$\begin{aligned} I(t) &= I_c(t)\sqrt{1-\eta^2(t)}\sin\phi(t) \\ \frac{\partial}{\partial t}\phi &= -\Delta\mu(\phi,\eta) \end{aligned} \tag{2}$$

with $\eta = \frac{N_2-N_1}{N_2+N_1}$, $I_c(t) = \Omega_R \int \mathrm{d}\boldsymbol{r}\Phi^2(\boldsymbol{r})\mathrm{e}^{\mathrm{i}p(t)z/\hbar}$, $p = p_1 - p_2$ and, in the far-detuned case, the chemical potential difference $\Delta\mu = \mu_1 - \mu_2 \simeq \delta$. We remark that the atomic current $I = \frac{\partial}{\partial t}\eta$ depends on the relative average phase $\phi(t) = \phi_1(t) - \phi_2(t)$. In the strong-coupling limit ($\delta \lesssim \Omega_R$), the two-mode approximation breaks down, and hence equations (2) cannot be retrieved.

Equations (2) are generalized Josephson equations, similar to those governing a voltage-driven superconducting junction [16]. Here, however, the critical current $I_c(t)$ depends explicitly on time due to the dynamical phase, $\mathrm{e}^{\frac{\mathrm{i}}{\hbar}p(t)z}$, accumulated by the two condensates. The spin dynamics can be decoupled from the much slower spatial dynamics so, to a good approximation, $p \simeq -mgt/2$. This gives a decreasing critical current $I_c(t) \approx \Omega_R\ \mathrm{e}^{-t^2/\Gamma^2}$ with a relaxation time $\Gamma \simeq 130$ μs. A further departure from the standard Josephson current relation is given by the term $\sqrt{1-\eta^2}$ [14], absent in superconducting systems where $\eta \approx 0$ [3] due to the presence of external circuits which suppress charge imbalances. In Figure 1a the time evolution of the fractional relative population observed experimentally is compared with the solution of the Josephson equations (2).

Response of the thermal gas

In order to highlight the macroscopic quantum nature of the condensate oscillations, we show that those of a non-condensate (thermal) atomic cloud, driven by the same external rf field, die out on a much shorter time scale. The difference between the two relaxation times is a manifestation of the BEC long-range order respect to the microscopic coherence length of the non-condensate cloud. Indeed, the relaxation of the condensate oscillation is purely dynamical (due to the different trapping potentials felt by the two Zeeman states), while the decay of the thermal gas is mainly due to a strong dephasing.

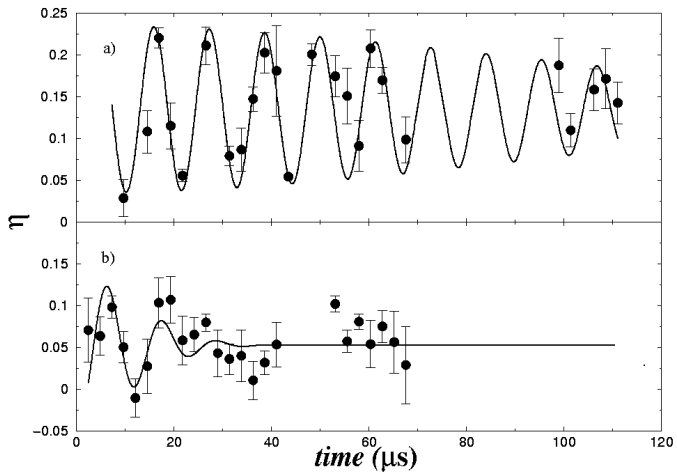

Fig. 2. a) Time evolution of the fractional relative population of the two condensates, $\eta = (N_2 - N_1)/(N_2 + N_1)$. The experimental data (dots) are compared with the theoretical prediction (solid line) as described in the text. N_2 and N_1 are, respectively, the number of particles in the Zeeman states $|F = 2, m_F = 2\rangle \equiv |2\rangle$ and $|F = 2, m_F = 1\rangle \equiv |1\rangle$. The condensate is initially created in the state $|2\rangle$ with typically $\approx 150,000$ atoms: a first $\pi/2$ pulse of 13 μs ($\Omega_R = 2\pi\times(26\pm2)$ kHz, $\delta = 0$) transfers half $|2\rangle$ population in the state $|1\rangle$. A second far-detuned pulse ($\Omega_R = 2\pi\times(13\pm2)$ kHz, $\delta = 2\pi\times(80\pm10)$ kHz) is applied after 4.0 ± 0.1 μs. At the end of the second pulse the trap is turned off, and the population of both condensates is destructively measured with laser imaging techniques. The frequency of the oscillations is $\nu = 88$ kHz, and the relaxation time is $\Gamma \simeq 130$ μs. b) Time evolution of the fractional relative population of the thermal clouds $\eta = (N_2 - N_1)/(N_2 + N_1)$. The temperature is $T \simeq 0.4$ μK $\simeq 3T_c$. Initially all thermal atoms are in the state $|2\rangle$ level, forming a Gaussian cloud with a width of 15 μm. As in Figure 1a, a first $\pi/2$ pulse transfers half $|2\rangle$ population in the state $|1\rangle$. After this pulse, the second far-detuned pulse is applied. The parameters of (and the time-delay between) the two pulses are the same as in Figure 1a. The theoretical frequency of the oscillations is $\nu = 88$ kHz, as for the condensate oscillations, while the relaxation time is $\Gamma \simeq 15$ μs, which has to be compared with the value (130 μs) for the condensate.

In our experiment, a thermal atomic cloud is initially trapped in the Zeeman level $|2\rangle$, at a temperature $T \simeq 3\ T_c$. In first approximation, the gas is very dilute and can be seen as a "swarm" of non-interacting particles. After the first $\pi/2$ pulse, the far-detuned rf field is applied, and the atomic population recorded. The oscillations die out in $\sim$40 μs Figure 2b, which should be compared with the $\sim$200 μs in which the condensate oscillations disappear. The density matrix is $\rho = \sum_\alpha \rho^{(\alpha)} = \sum_\alpha |\psi^{(\alpha)}\rangle \langle\psi^{(\alpha)}|$, where α runs over the number of particles and $\langle\psi^{(\alpha)}| = \left(\sum_n a_n^{(\alpha)*} \mathrm{e}^{-\mathrm{i}p_1 z/\hbar}\langle\varphi_n|\ ,\ \sum_m b_m^{(\alpha)*}\mathrm{e}^{-\mathrm{i}p_2 z/\hbar}\langle\varphi_m|\right)$, with $\{|\varphi_n\rangle\}$ a complete basis of H_2 with eigenvalues ϵ_n.

The Liouville-von Neumann equation for the density matrix gives the following equations for the a and b amplitudes:

$$\begin{aligned} \mathrm{i}\hbar\dot{a}_n^{(\alpha)} &\simeq (\epsilon_n + \frac{\hbar\delta}{2})a_n^{(\alpha)} + \frac{1}{2}\sum_m \hbar\Omega_{nm}(t) b_m^{(\alpha)} \\ \mathrm{i}\hbar\dot{b}_n^{(\alpha)} &\simeq (\epsilon_n - \frac{\hbar\delta}{2})b_n^{(\alpha)} + \frac{1}{2}\sum_m \hbar\Omega_{mn}^*(t) a_m^{(\alpha)} \end{aligned} \quad (3)$$

(we neglected terms small in respect to $\hbar\delta$). The transfer matrix elements are calculated as overlap integrals of the two-species wave-functions $\Omega_{nm}(t) = \Omega_R \int \mathrm{d}\boldsymbol{r}\varphi_n(\boldsymbol{r})\varphi_m(\boldsymbol{r})\mathrm{e}^{\mathrm{i}p(t)z/\hbar}$ (where $p = p_1 - p_2$). The orthogonality of the wavefunctions is gradually lost so, after a transient time, the diagonal and non-diagonal matrix elements become comparable, allowing for an incoherent exchange between states of different quantum numbers and, therefore, leading to a strong dephasing of the thermal oscillations. From our simulations $\Omega_{n,n} \sim \Omega_{n,n\pm1}$ at $t \sim 30$ μs.

We observe that, if the two trapping potentials were the same, all diagonal matrix elements in equations (3) would be equal to $\Omega_{nn} = \Omega_R$, while the off-diagonal terms would vanish ($\Omega_{nm} = 0$). Therefore the thermal cloud would exhibit undamped Rabi oscillations [17], indistinguishable from the condensate Josephson oscillations. In Figure 1b we show the time evolution of the relative population of the two thermal clouds, which is in fairly good agreement with our predictions.

Before concluding we want to stress that in the strong-coupling case ($\delta \gtrsim \Omega_R$), the dephasing times of condensate and thermal gases are different mainly because they have different dimensions [18]. Indeed $|1\rangle$ along the z-axis feels the potential $V_1 = \frac{1}{2}m\omega^2 l^2 z^2$, but it is initially in the center of the potential V_2, *i.e.* in $z_0 \approx 15$ μm. The gradient G of the magnetic potential in z_0 is $G = \frac{V'(z_0)}{2\pi\hbar} = \frac{m\omega^2 l^2}{4\pi\hbar} z_0 \approx 11$ MHz/cm. The phase of condensate $|j\rangle$ is now a function $\phi_j(z,t)$: in other words, the effective Rabi frequency depends on the spatial coordinate z. At a time τ of order $1/GL$, ($\tau \approx 220$ μs with $L \approx 4$ μm for the condensate and $\tau \approx 30$ μs with $L \approx 30$ μm for the thermal cloud), the phases (and the local relative phase $\phi = \phi_1 - \phi_2$) are spatially oscillating functions. At the same time τ, $\int \mathrm{d}z\phi(z,\tau) \approx 0$ and there is not longer a *net* transfer of particles. When the detuning δ is much greater than the Rabi frequency Ω_R (as in our experiment), $\phi_{2,1}(z,\tau) \approx \pm\frac{\delta}{2}$ plus an oscillating function. Then $\int \mathrm{d}z\phi(z,\tau) \neq 0$ and there is a net transfer of particles. Therefore, provided that the detuning is large enough, the width L does not affect the dephasing time. Furthermore, the phases $\phi_{1,2}$ does not depend on z: the spatially-dependent Rabi frequency is a weak perturbation of the detuning δ, as it should in a weak link.

Conclusions

The theoretical and experimental results here reported allow us to conclude that: 1) the far-detuned rf field behaves

like a superfluid weak link, 2) the current-phase dynamics is governed by generalized Josephson equations, and 3) the persistence of condensate oscillations for times much longer than those of the thermal cloud yields a clear signature of the macroscopic quantum coherence in Bose-Einstein condensates.

Our experimental setup would also enable one to study the analogous of several phenomena present in superconducting and superfluid Josephson junctions [19], as well as to address problems in the foundation of quantum mechanics, like the possibility to define a phase standard [20]. This might be investigated populating all the Zeeman sublevels, thus creating an array of Josephson junctions, whose relative phases can be properly manipulated by tuning the external rf field.

Furthermore, the comparison between the condensate and normal components of an atomic gas opens a new experimental way to testing theories of decoherence and dephasing mechanisms [10,21,22] by studying the Josephson dynamics of a condensate embedded in a thermal bath.

We thank M. Artoni, M. Modugno, M. Rasetti and S.R. Shenoy, for useful discussions. A.S., A.T. and T.L. wish to thank the LENS for the kind hospitality during the preparation of this work. This work has been partially supported by the Cofinanziamento MURST, by the EU under Contracts No. HPRI-CT 1999-00111 and by the INFM Progetto di Ricerca Avanzata "Photon Matter". T.L. has been supported by the European Science Foundation (ESF).

References

1. D.R. Tilley, J. Tilley, *Superfluidity and Superconductivity* (Hilger, New York 1990)
2. B.D. Josephson, Phys. Lett. **1**, 251 (1962)
3. A. Barone, G. Paternó, *Physics and Applications of the Josephson Effect* (Wiley, New York, 1982)
4. O. Avenel, E. Varoquaux, Phys. Rev. Lett. **60**, 416 (1988)
5. S.V. Pereverzev, S. Backaus, A. Loshak, J.C. Davis, R.E. Packard, Nature **388**, 449 (1997)
6. B.P. Anderson, M.A. Kasevich, Science **282**, 1686 (1998)
7. F.S. Cataliotti, S. Burger, C. Fort, P. Maddaloni, F. Minardi, A. Trombettoni, A. Smerzi, M. Inguscio, Science **293**, 843 (2001)
8. J.E. Williams, Phys. Rev. A **64**, 013610 (2001)
9. R.A. Webb, R.L. Kleinberg, J.C. Wheatley, Phys. Lett. A **48**, 421 (1974)
10. A.J. Leggett, Rev. Mod. Phys. **73**, 307 (2001)
11. F. Dalfovo, S. Giorgini, L.P. Pitaevskii, S. Stringari, Rev. Mod. Phys. **71**, 463 (1999)
12. P. Maddaloni, M. Modugno, C. Fort, F. Minardi, M. Inguscio, Phys. Rev. Lett. **85**, 2413 (2000)
13. J. Williams, R. Walser, J. Cooper, E. Cornell, M. Holland, Phys. Rev. A **59**, R31 (1999)
14. A. Smerzi, S. Fantoni, S. Giovannazzi, S.R. Shenoy, Phys. Rev. Lett. **79**, 4950 (1997); S. Raghavan, A. Smerzi, S. Fantoni, S.R. Shenoy, Phys. Rev. A **59**, 620 (1999)
15. C. Cohen-Tannoudji, B. Diu, F. Laloe, *Quantum Mechanics*, Vols. 1, 2 (New York, Wiley, 1977)
16. R.P. Feynman, *The Feynman Lectures on Physics* (Addison Wesley, New York, 1965)
17. N.F. Ramsey, *Molecular Beams* (Oxford Press, 1985)
18. F. Minardi, C. Fort, P. Maddaloni, M. Modugno, M. Inguscio, Phys. Rev. Lett. **87**, 170401 (2001)
19. A. Barone, in *Quantum Mesoscopic Phenomena and Mesoscopic Devices in Microelectronic*, edited by I.O. Kulik, R. Ellialtioglu (Kluwer Academic Publishers, Netherlands, 2000), p. 301
20. A.J. Leggett, in *Bose-Einstein Condensation*, edited by A. Griffin, D.W. Snoke, S. Stringari (Cambridge University Press, Cambridge, 1995), p. 452
21. J. Ruostekoski, D.F. Walls, Phys. Rev. A **58**, R50 (1998)
22. W. Zurek, Phys. Today **44**, 36 (1991)